Infrared Molecular Line Profiles from Dynamical Models for Circumstellar Dust Shells around Long–period Variables

JAN MARTIN WINTERS[1], JOHN J. KEADY[2],
AXEL J. FLEISCHER[1], ANDREAS GAUGER[2]

[1] Institut f. Astronomie & Astrophysik, TU Berlin, Germany
[2] Los Alamos National Laboratory, Group T4, New Mexico, USA

Poster contribution presented at *A half century of stellar pulsation interpretations: A tribute to Arthur N. Cox* , June 16–20 1997, Los Alamos, New Mexico

1 Introduction

Long–period Variables are highly evolved low and intermediate mass stars located on the Asymptotic Giant Branch (AGB) in the Hertzsprung–Russell diagram. These objects are large amplitude pulsators with typical periods of the order of 1 yr, high luminosities $\approx 10^4 \mathrm{L}_\odot$, and low effective temperatures $< 3000K$. During this evolutionary state, the stars develop massive circumstellar shells which expand at typical velocities of $\approx 15\,\mathrm{km\ s}^{-1}$, thereby carrying high mass loss rates up to $10^{-4}\mathrm{M}_\odot\mathrm{yr}^{-1}$ (Loup et al. 1993).

The outflows from these cool stars are sites of effective grain formation, indicated by a substantial reddening of the stellar radiation field and by the occurrence of characteristic dust features in the spectra of the circumstellar shells.

In order to study the structure and dynamics of such circumstellar dust shells (CDS), the CO molecule is an especially well suited diagnostic probe. It is one of the most abundant species, both, in oxygen–rich and in carbon–rich objects. Due to its stability it forms already at high temperatures deep in the photosphere. In the subsequent outflow it remains relatively chemically inert out to large distances, thus, covering the whole range of conditions in the CDS. Its infrared and microwave spectrum is fairly simple, and line positions and oscillator strengths are well determined.

We have performed non-LTE radiative transfer calculations for CO infrared lines, using the structure of a dynamical dust shell model. The resulting line profiles are compared to high resolution CO line spectra obtained from the carbon–rich Mira IRC+10216 at the KPNO Mayall 4m telescope.

2 Time–dependent hydrodynamical model calculation

We consider a spherically symmetric shell around a Red Giant, characterized by its mass $M_\star$, effective temperature $T_\star$, luminosity $L_\star$, and photospheric element abundances ϵ_i. The pulsation of the star is simulated by a sinusoidally moving inner boundary, described by the period P and velocity amplitude Δv_P.

Our approach is described in detail in Fleischer et al. (1992).

These models comprise a consistent treatment of hydrodynamics, thermodynamics, continuum radiative transfer, chemistry, and carbon grain formation. The formation, growth, and evaporation of dust particles is calculated by means of a moment method (Gail & Sedlmayr 1988, Gauger et al. 1990), which includes an equilibrium chemistry for the important hydrocarbons.

3 Molecular line calculations

The synthetic infrared CO line profiles are calculated using the radial structure for the density and temperature of the gas and the dust, which result from these dynamical model calculations.

Line radiative transfer is calculated by integrating the formal solution of the observers frame radiation transport equation along the characteristic rays to yield the emergent intensity, from which the flux profiles are calculated. Previous non–LTE calculations indicated, that the CO vibrational level populations are essentially in equilibrium at the dust temperature for optically thick dust shells. Therefore, in the present calculations the vibrational level populations are determined from a Boltzmann distribution at the dust temperature.

A detailed description is given in (Keady 1982).

4 Structure of the dust shell model

The values adopted for the present dust shell model are

$L_\star$	=	8000 $L_\odot$
$T_\star$	=	3000 K
ϵ_C/ϵ_O	=	1.30
$M_\star$	=	0.8 $M_\odot$
P	=	650 d
Δv_P	=	8.0 km s^{-1}

which results in a calculated

- final outflow velocity = 13.5 km s^{-1}
- mass loss rate = 3.5 10^{-5} $M_\odot$ yr^{-1}
- dust–to–gas ratio = 1.2 10^{-3}

The radial structure of this dynamical dust shell model is shown in Fig. 1 for one instant during the cycle.

The process of dust formation depends sensitively on the local temperature and density, which vary substantially in the inner parts of the atmosphere due to the passage of shocks generated by the interior pulsation. Therefore, grains can form only in a limited radius interval and during certain phases of the cycle. On the other hand the grains decisively affect the hydro– and thermodynamic structure of the flow. This interaction leads to a variety of **dust induced dynamical phenomena** (Fleischer et al. 1992):

> Inhomogeneous shell–like distribution of the circumstellar dust caused by the variation of temperature, density, and chemical composition in the dust forming region.
>
> Strong shocks dominating the shell structure, either generated by pulsation and amplified by radiation pressure on newly formed grains, or even produced by radiation pressure alone.
>
> Substantial backwarming of the atmosphere inside the dust forming region due to the dust opacity, where in turn the temperature increase terminates condensation.

In this model dust is formed on a time scale longer than the pulsation cycle. Fleischer et al. (1995) showed, that the dust shell is controlled by a time scale of its own, which differs from the time scale of the interior pulsation. This time scale is decisively influenced by the carbon abundance, and depending on its value, the models show a spatial structure repeating after one period, or after multiples of the period, or which even do not repeat at all, but show an irregular behavior, as in the model presented here.
The spatial structure of our dust shell models and its time variation manifests itself in the optical appearance (Winters et al. 1994, 1995):

- Shifts of the amplitude and the average magnitude of the synthetic light curves
- Step-like structures in the synthetic brightness profiles

5 Synthetic line profiles

The synthetic infrared CO $v = 0-2$ R8 overtone line profile is shown in Fig. 2 for different instants of time. Around $t = 72$P an absorption feature starts to develop at $\approx 5\,\mathrm{km s^{-1}}$. This feature considerably increases in strength during the following time interval and simultaneously shifts to higher velocities. The dominant core of the profile at $\approx 15\,\mathrm{km s^{-1}}$ is saturated during most of the time interval shown.

> The temporal evolution of the secondary feature is caused by the formation of a new dust layer:

In Fig. 3 the radial structure of the model is shown at $t = 72.25\,\mathrm{P}$ and at $t = 73.25\,\mathrm{P}$, i.e. at two phases enclosing the occurrence of the low–velocity absorption feature. In this time interval, a new dust layer starts to develop in the region around $5R_0$. Radiation pressure acting on this layer leads to the acceleration of a dust amplified shock and to an enhanced density and temperature in the region around $5R_0$ (dashed curves in Fig. 3).

The shock velocity slowly increases during the following time interval. Simultaneously, a second dust layer develops in the wake of this shock. These two new dust layers can be seen in the region between 5 and $10R_0$ in Fig. 1 (at $t = 75.25$P).

6 Comparison with IRC +10216

The l.h.s. column of Fig. 4 displays the temporal evolution of the observed 2-0 overtone line profile in IRC +10216. The dates of observation are separated by ≈ 2.5P and ≈ 3.2P, where P (= 650d) is the pulsation period of IRC +10216.

Note, that the observed line cores are **not** saturated.

In the r.h.s. column of Fig. 4, the temporal evolution of the calculated profile is displayed again for comparison. Here, the CO abundance in the model has been reduced artificially by a factor of 0.33 in order to approximate the observed strength of the line core.

The low–velocity absorption feature in the synthetic and the observed profile evolves on about the same time scale.

7 Conclusions

The comparison of synthetic infrared CO line profiles calculated on the basis of a time-dependent dust shell model with the corresponding lines observed in IRC+10216 shows, that the model calculations yield a dynamical behavior capable of explaining the long term variations and the line core positions seen in the observed low excitation first overtone profiles.

However, the calculated first overtone line strengths are too high, indicating that the CO density and thus possibly the mass loss rate of the model is too high and should be closer to a value of
$\approx 1 \cdot 10^{-5}\ \mathrm{M}_\odot/\mathrm{yr}$.

Other possibilities influencing the line strength:

Chemical non–equilibrium effects on the CO density, e.g. by photo–dissociation in radiating shocks

Effects caused by the well known aspherical geometry of the inner shell region of IRC +10216

Acknowledgments
This work has been supported by the Deutsche Forschungsgemeinschaft (grant Se 420/5–4) and by the BMBF (grant 05 3BT13A 6). Research at Los Alamos National Laboratory was performed under the auspices of the U.S. Department of Energy.

References

Fleischer A. J., Gauger A., Sedlmayr E., 1992, A&A 266, 321–339
Fleischer A. J., Gauger A., Sedlmayr E., 1995, A&A 297, 543–555
Gail H.-P., Sedlmayr E., 1988, A&A 206, 153–168
Gauger A., Gail H.-P., Sedlmayr E., 1990, A&A 235, 345–361
Keady J. J., 1982, The circumstellar envelope of IRC +10216, PhD thesis, New Mexico State University, Las Cruces, New Mexico
Loup C., Forveille T., Omont A., Paul J. F., 1993, A&AS 99, 291–377
Sada P. A. V., 1993, Temporal variations in the circumstellar shell IRC +10216, PhD thesis, New Mexico State University, Las Cruces, New Mexico
Winters J. M., Fleischer A. J., Gauger A., Sedlmayr E., 1994, A&A 290, 623–633
Winters J. M., Fleischer A. J., Gauger A., Sedlmayr E., 1995, A&A 302, 483–496

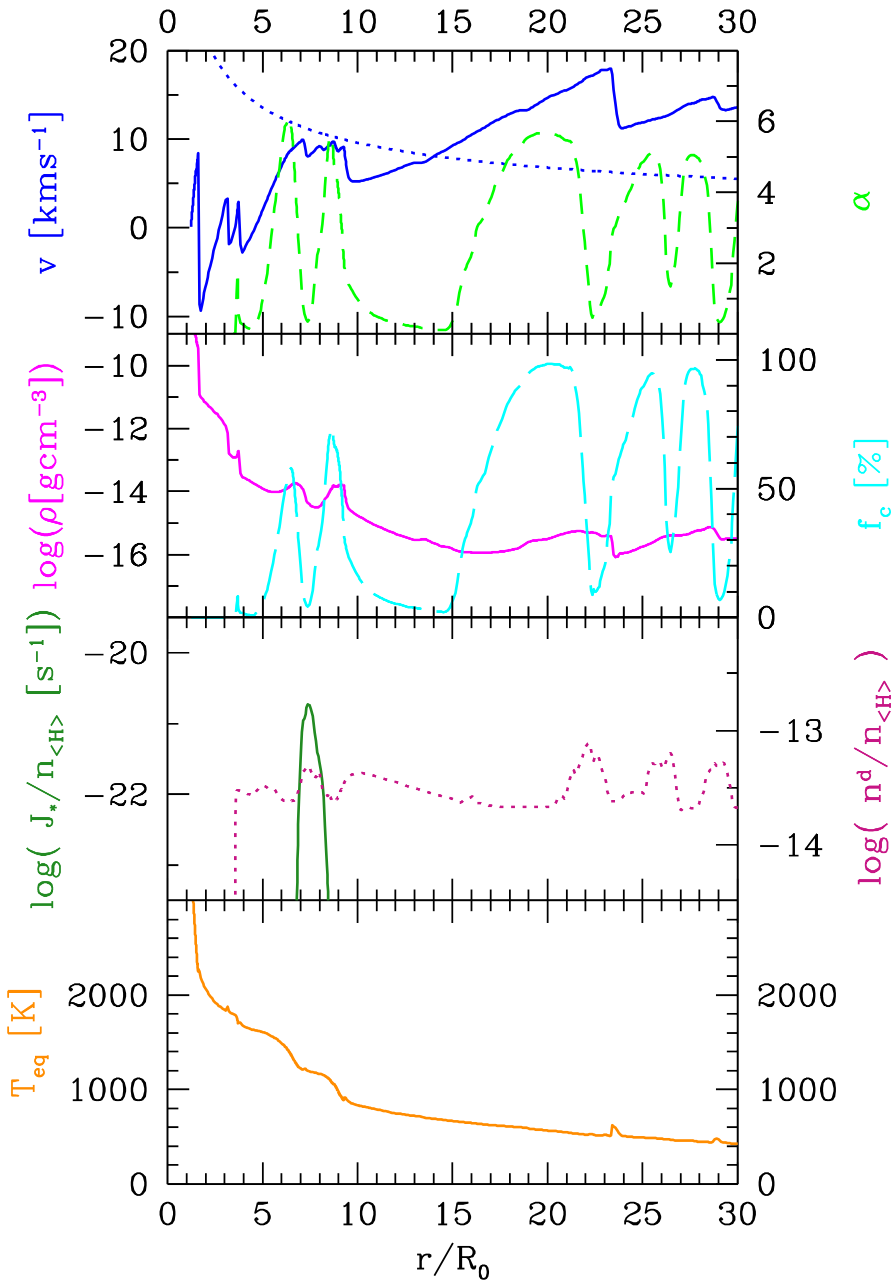

Figure 1: Radial structure of the dust shell model at $t = 75.25$P.
upper diagram: velocity v (solid line), escape velocity (dotted line), and radiative acceleration α (dashed line),
2nd diagram: density ρ (solid line) and degree of condensation f_c (fraction of actually condensed carbon) (dashed line),
3rd diagram: nucleation rate $J_\star$, i.e. the number of dust particles formed per second and H-atom (solid line) and number of dust particles per H–atom $n_{\rm d}/n_{<\rm H>}$ (dotted line),
lower diagram: equilibrium temperature $T_{\rm eq}$.

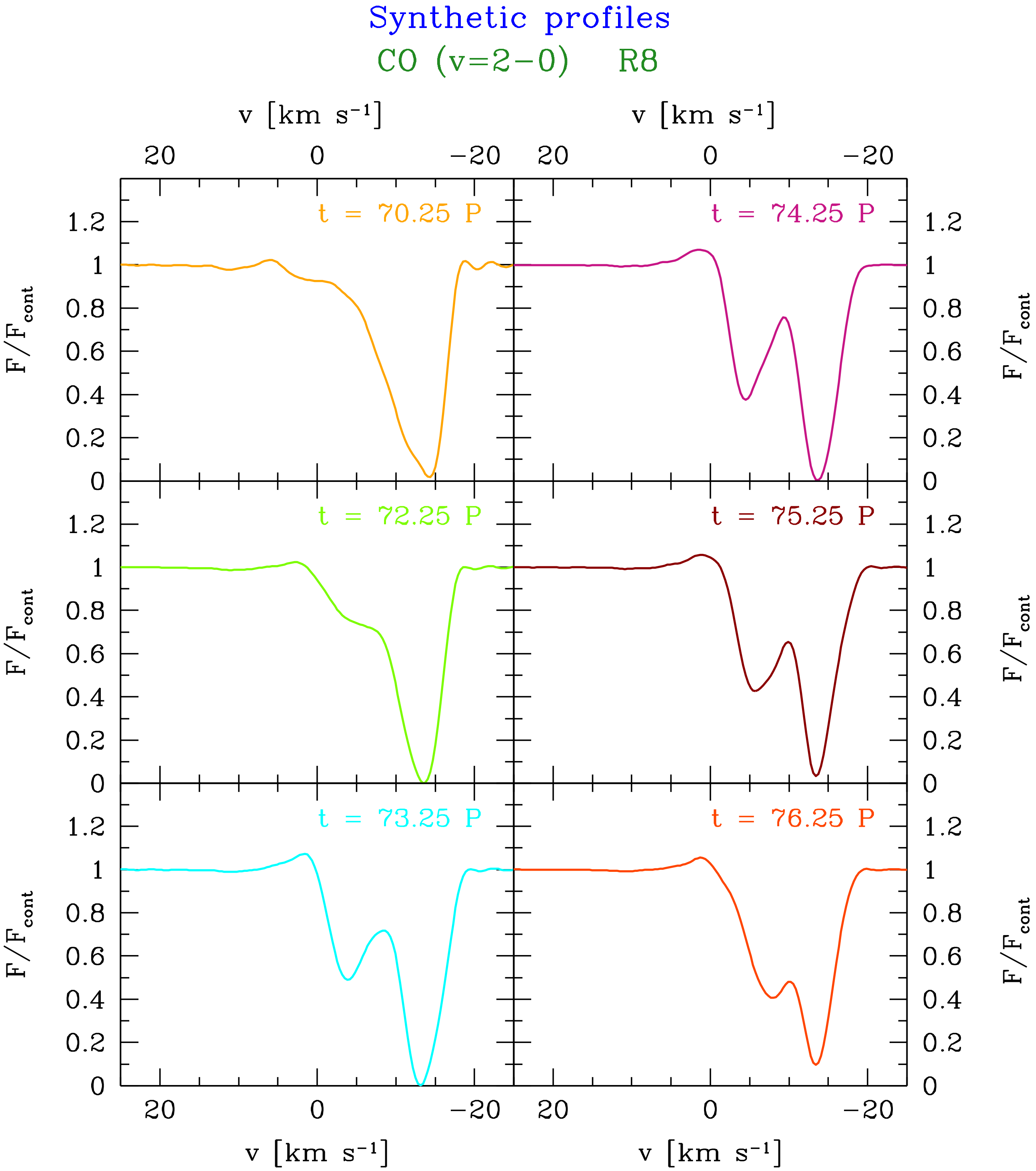

Figure 2: Synthetic CO ($v = 2 - 0$) first overtone line profiles at different instants of time. Note that a strong absorption feature evolves around $5\,\mathrm{kms}^{-1}$ between $t = 70.25$P and $t = 73.25$P.

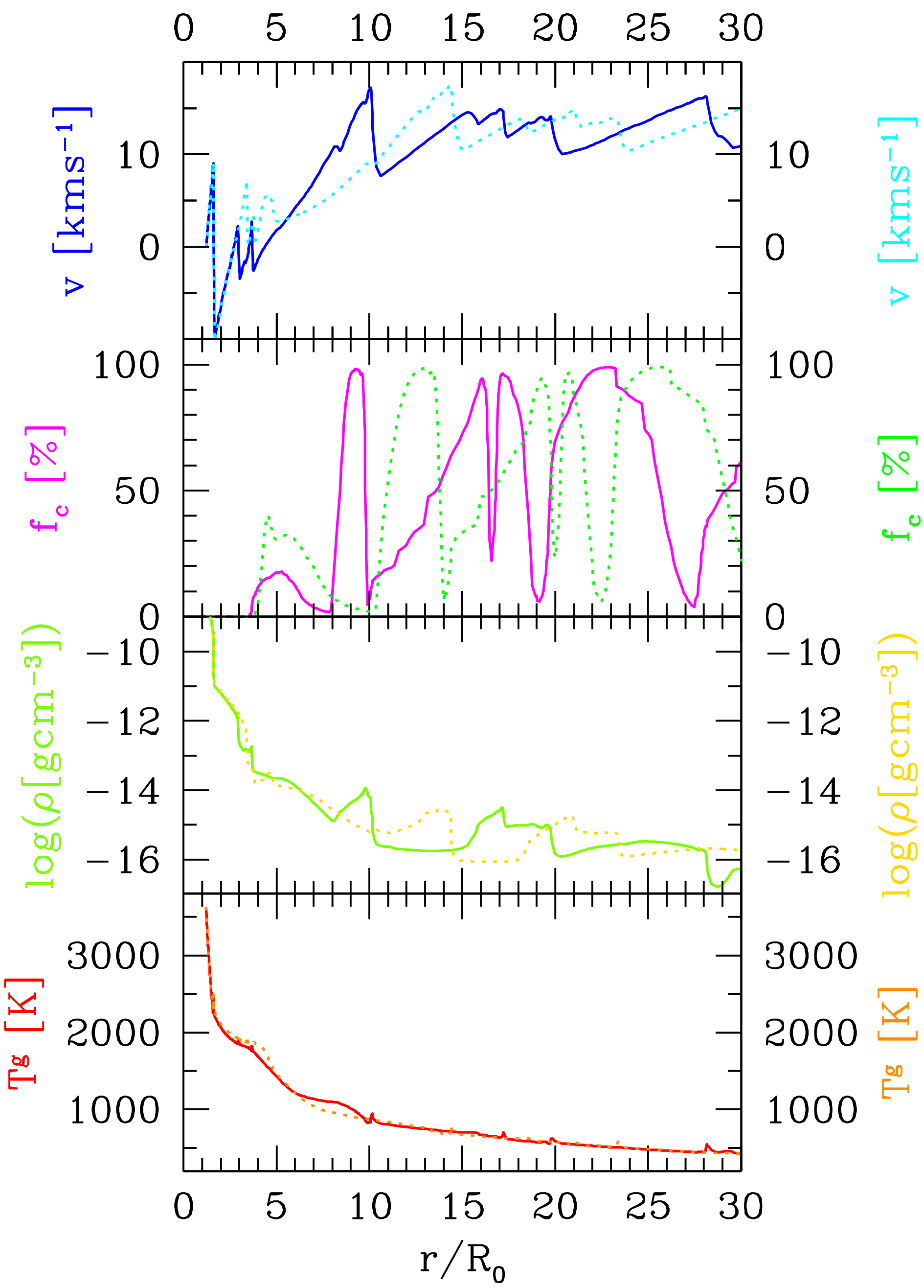

Figure 3: Radial structure of the model at t = 72.25P (solid lines) and at t = 73.25 (dashed lines). Note the enhanced density and temperature, and the new stronger shock in the region around $4\,R_0$ at $t = 73.25$.

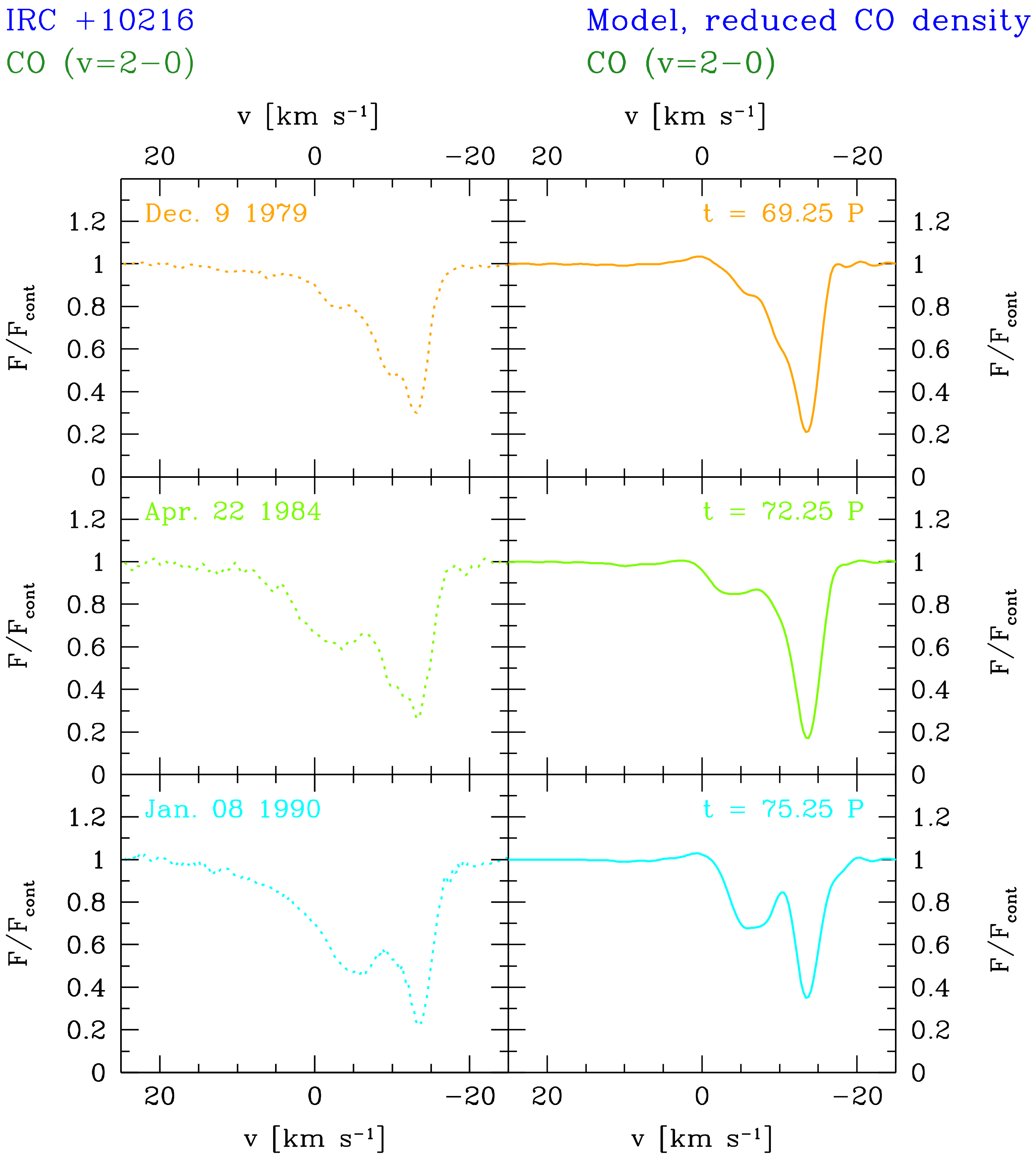

Figure 4: Temporal variation of low excitation CO 1st. overtone lines.
l.h.s. column: observed profiles of IRC +10216 (Sada 1993)
r.h.s. column: calculated profiles The CO concentration is reduced by a factor of 0.33.